Human dilated ascending aorta: mechanical characterization *via* uniaxial tensile tests

A. Ferrara[a,*], S. Morganti[b], P. Totaro[c], A. Mazzola[c], F. Auricchio[a]

[a]*Dipartimento di Ingegneria Civile e Architettura (DICAr), Università degli Studi di Pavia, Pavia, Italy*
[b]*Dipartimento di Ingegneria Industriale e dell'Informazione (DIII), Università degli Studi di Pavia, Pavia, Italy*
[c]*Dipartimento Cardio-Toraco-Vascolare, IRCCS Policlinico San Matteo, Pavia, Italy*

Abstract

Aneurysms of the ascending aorta (AsAA), i.e., a progressive and localized dilatation of the first part of the aorta, represent a severe life-threating condition, often occurring without any symptom. AsAA formation is associated with a degeneration of the aortic wall tissue, which leads to changes in the tissue mechanical properties, and in particular to increased wall stress and/or a decreased wall ultimate strength. Up to now, the decision to surgically operate is usually based on the AsAA diameter, although such a criterion is not always predictive.

The present study focuses on the characterization of the mechanical behavior of the AsAA tissue. Specimens were cut from portions of dilated ascending aorta excised from 46 patients through open-heart surgery. Peak strain, peak stress and maximum elastic modulus (i.e., tissue stiffness) were measured from uniaxial stress-strain curves. Such mechanical properties were collected for different regions of the aortic wall (anterior and posterior) as well as for different specimen orientations (circumferential and longitudinal). Relationships of ultimate mechanical properties with patient age and sex were also investigated.

The obtained results confirm the anisotropic behavior of healthy tissues, highlighting a significant anisotropy of the AsAA tissue, with higher value of strength and stiffness in the circumferential than in the longitudinal direction. Higher strength and stiffness were also found in the posterior region than the anterior one for the circumferential orientation, whereas an opposite result was found for the longitudinal orientation. A decreasing trend of ultimate mechanical properties with aging was also highlighted. Finally, a significant difference in the strength between males and females was observed only in the circumferential direction.

Keywords: Ascending aorta aneurysm, Dilated aorta, ultimate mechanical properties, uniaxial tensile tests.

1. Introduction

Cardiovascular diseases such as aneurysm, atherosclerosis and dissection, are caused by significant alterations in the arterial wall tissue and represent the leading cause of death in the western countries [1, 2]. Among them, aneurysms of the ascending aorta (AsAA), i.e, a progressive dilatation of the first part of aorta, represent a severe life-threating condition since patients often remain asymptomatic until dissection or rupture. The incidence of AsAA has been estimated in about 5-10 cases per 100000/year, with a peak during the sixth and seventh decade of life [3–5].

If on one hand, the high risk of rupture increases unequivocally with aging, on the other hand, the concomitant presence of co-morbidities, including genetic mutations (Marfan synmdrome) [6–8], connective tissue disorders (Ehler Danlos disorders) [9, 10], and congenital cardiovascular conditions (bicuspid aortic valve) [11–14], can favor aneurysm rupture also in younger subjects.

Up to now, the only treatment option for the AsAA disease is the replacement of the dilated part of the ascending aorta by surgical repair [15–18]. Since any open-heart surgical intervention involves non-negligible risks, it is important to establish the trade-off between the risk for aneurysm rupture and the risk of surgical repair. The decision to surgically operate is usually based on the maximum diameter criterion, i.e., patients with an ascending aorta dilated up to 5.5 cm are considered at high risk for rupture and, consequently, recommended for surgical replacement [19, 20]. However, such a criterion is not always predictive: in fact, aneurysm rupture is known to occur also at lower diameters as well as in presence of co-morbidities. For such cases, the diameter threshold can decrease until to 4.5 cm [18, 20]. Accordingly, it follows the necessity to define more exact guidelines to support cardiologists in predicting adverse events and to guide the decision process before surgical intervention.

It is known that aneurysm formation is associated with changes in the content and architecture of elastin and collagen fibers within the aortic tissue [21–24]. Such a tissue degeneration leads to changes in the tissue mechanical properties, which induce increased wall stress and/or a decreased wall ultimate strength [25]. Moving from such considerations, the bio-mechanical characterization of dilated ascending aorta tissues appears to be helpful for understanding the stage of the aortic disease, and then, the potential risk for aneurysm rupture.

Different works available in the literature prove the increased interest of researchers on the bio-mechanical

*Corresponding author
Email address: anna.ferrara@unipv.it (A. Ferrara)

characterization of dilated ascending aorta. In particular, some studies move from the presentation of new tools in imaging analysis to evidence possible alterations in the morphology and in the micro-structure of the diseased aortic tissues [26, 27]. Other studies focus on the use of mechanical tests (uniaxial and biaxial tensile tests) to evaluate and compare mechanical properties of both healthy and diseased tissues [28–33] and, at the same time, to investigate factors which can influence the tissue properties like location and orientation [23, 34–37], patient age [30, 38, 39], patient sex [39, 40] and presence of concomitant pathologies [25, 33, 36, 41–44].

However, a unique methodological procedure to be adopted for mechanical tests on human aortic tissues has not been defined and accepted yet. Consequently, the reported experimental results are often not comparable and, sometimes, even conflicting. The possibility to define in a more precise manner the mechanical properties of dilated ascending aorta for accurate and firm conclusion thus remains a challenge for both researchers and intervention cardiologists.

To the authors' knowledge, the experimental data available for AsAA are still limited (in comparison, for example, with the ones for abdominal aorta aneurysm), so that one of the goal of the present work is to significantly improve the collection of mechanical data on human dilated ascending aorta up to now available in the literature and, then, to extrapolate information on how such data can be influenced by tissue location and orientation as well as patient age and sex. A constant interaction and collaboration between an engineering unit of the Department of Civil Engineering and Architecture of the University of Pavia, Italy, and a Heart-Surgery unit of the IRCCS Policlinico San Matteo of Pavia made the present work possible.

In the following, the organization of the paper is briefly presented. Section 2 starts with a description of the methodology adopted for preparation and testing of the specimens of human dilated ascending aorta. Then, the post-processing technique used for both data and statistical analysis are described. Finally, Section 3 summarizes the experimental results, which are subsequently discussed in Section 4.

2. Materials and method

A standard protocol was systematically adopted for collection, preparation and testing specimens of human dilated ascending aorta and for post-processing the obtained data. In the following, each step of the adopted procedure is detailed.

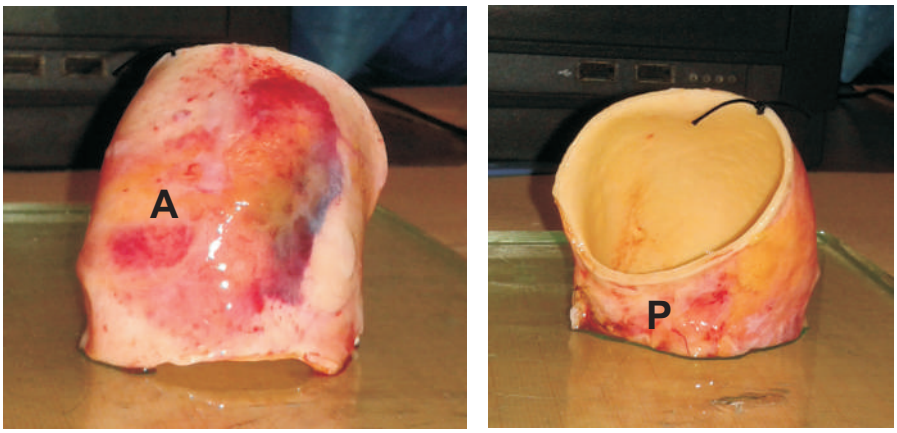

(a) (b)

Figure 1: Representative pictures of an excised part of dilated ascending aorta where two region may be distinguished: (a) anterior region, A, and (b) posterior region, P.

2.1. Sample collection and specimen preparation

Tubular portions of dilated ascending aorta, see Figure 1, were excised from 46 patients (34 male and 12 female, with average age 62 ± 14 years) who underwent elective AsAA surgical repair at IRCCS Policlinico San Matteo of Pavia, Italy, between May 2013 and December 2014. Informed consent was provided in all considered cases.

As shown in Figure 1, two regions can be distinguished in the excised AsAA part, i.e., the anterior and posterior one. In particular, the anterior region corresponds to the part with lower curvature, and the posterior region to the part with higher curvature. Consequently, the original tube-shaped AsAA part was cut into two samples corresponding to the anterior and posterior region, respectively (see Figure 2(a)). After excision, the aortic samples were stored in isotonic physiological solution and kept in a refrigerator at 4^{o}C until mechanical testing.

Specimen preparation and mechanical testing were performed at the Department of Civil Engineering and Architecture of the University of Pavia, within 48 hours from the sample collection. After equilibration at room temperature surrounding adipose and connective tissues were removed from the collected aortic samples. Then, multiple bone-shaped specimens, whose number depends on the original size of the excised sample, were circumferentially and longitudinally cut using ad-hoc developed pattern blades, see Figure 2(b). Black-color lines drawn in the middle part of the specimen were used as gauge markers for

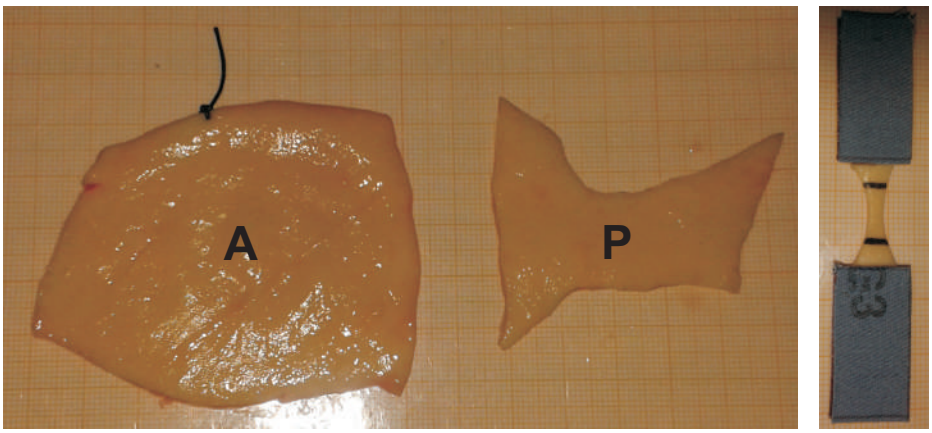

(a) (b)

Figure 2: Preparation of ascending aorta specimens for uniaxial testing. (a) Anterior and posterior sample (A and P) cut from the original tube-shaped AsAA. (b) Specimen with markers and grit sandpapers, ready for testing.

extension measurements. Adhesive sandpaper of fine grit was placed at both ends of each specimen with a super-adhesive gel in order to ensure clamping in the tensile-test machine and prevent slipping during mechanical testing.

For each specimen, the following dimensions were measured: i) the initial width of the narrowest section, w_0, ii) the initial thickness at three different points of the specimen, which were averaged to obtain the representative thickness, t_0, iii) the initial distance between the two markers, d_0, and iii) the distance between the two grips once positioned the specimen, l_0. The product of w_0 and t_0 was used to compute the initial cross-sectional area, $A_0 = w_0 \cdot t_0$.

2.2. Mechanical tests

Mechanical tests were performed using the MTS Insight Testing System 10 kN (MTS System Corporation) consisting of an electro-mechanical two-columns load frame with a moving solid steel cross-head. The MTS system is equipped with a 250 N load-cell (rated force capacity, 250 N) anchored to the cross-head and by two pneumatic grips, both suitable for testing soft tissues. The air pressure of the grips was fixed to 20 psi to prevent tissue crushing and, at the same time, specimen slipping. Finally, the specimen extension (i.e., the progressive changes in marker distance) was measured using the ME-46 Video Extensometer (resolution: 1 micron; camera field of view: 200 mm).

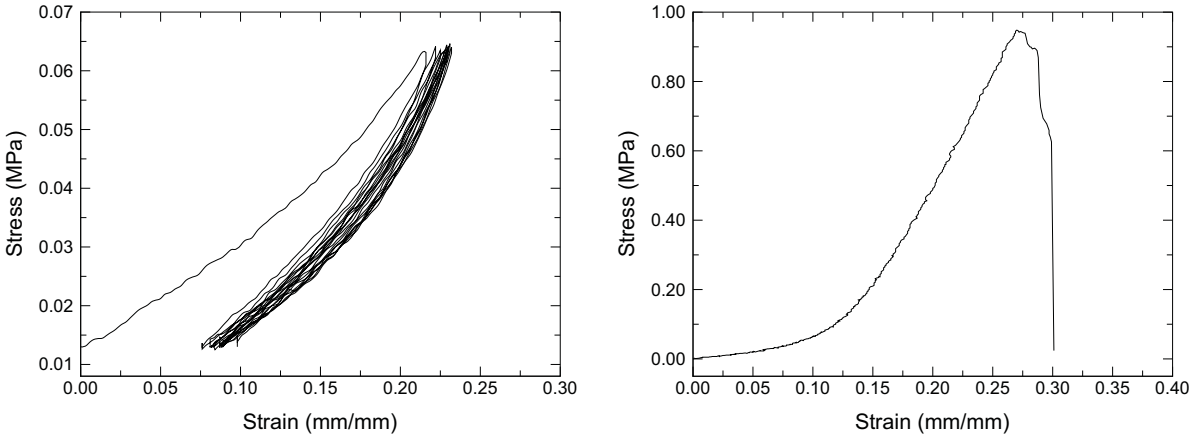

(a) Representative preconditioning response

(b) Representative uniaxial tensile response

Figure 3: Representative stress-strain curves recorded by the TestWork4 (TWS4): (a) preconditioning; (b) uniaxial tensile test.

The mechanical testing procedure was performed in two subsequent steps: i) preconditioning to stabilize the specimens and to obtain repeatable stress-strain curves; and ii) uniaxial tensile extension to characterize the mechanical response of the aortic tissue. Preconditioning was achieved executing 10 successive loading-unloading cycles at a constant cross-head speed of 10 mm/min from a minimum load of 0.1 N to a maximum of 0.50 N, see Figure 3(a). Uniaxial tensile extension were performed at the same cross-head speed of 10 mm/min until specimen rupture, see Figure 3(b). During preconditioning and extension, load and displacement were continuously recorded with a sampling frequency of 10 Hz.

Two representative pictures of fractured specimens are shown in Figure 4, which highlights typical types of specimen rupture occurred during the testing procedure, i.e., either inside the two markers, see Figure 4(a), or outside the two markers and close to one of the two grips, see Figure 4(b). Only specimens broken inside the two markers were considered as successful tests and included in our study.

2.3. Post-processing

The only experimental data corresponding to successful tests were collected and analyzed in the post-processing step, which includes data analysis, curve fitting with elastic modulus computation and statistical analysis. In the following, each phase of the post-processing step is detailed.

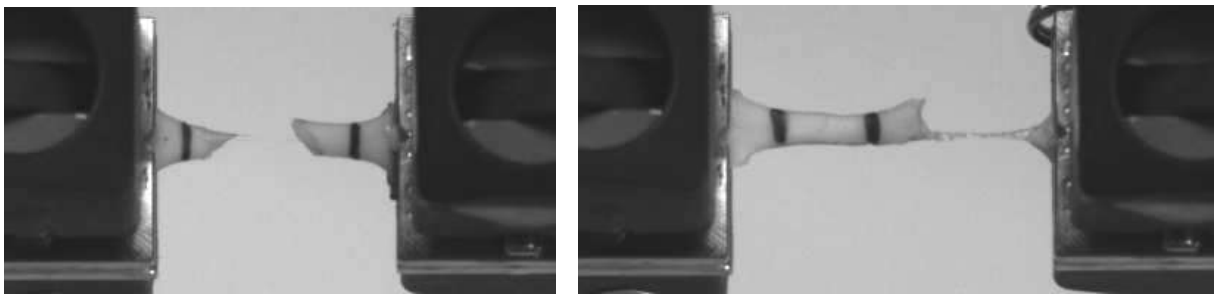

(a) Successful test (b) Unsuccessful test

Figure 4: Representative pictures of fractured tissue specimens. (a) Rupture occurred inside markers (successful test). (b) Rupture occurred outside markers and close to a grip (unsuccessful test).

2.3.1. Data analysis

Data analysis included the computation of stress, strain and elastic modulus from the quantities directly recorded during the mechanical testing, i.e., the tensile load, F, provided by the load cell and the specimen extension, Δd, measured by the video extensometer.

The load and elongation data were post-processed with Matlab R2011 (The MathWorks, Inc., Natick, MA, U.S.A.) to compute the *engineering* stress, σ_{E}, and the *engineering* strain, ε_{E}, defined in terms of the initial cross-sectional area and the initial length of the specimen, A_0 and d_0, respectively:

$$\sigma_{\mathrm{E}} = \frac{F}{A_0}, \qquad \varepsilon_{\mathrm{E}} = \frac{\Delta d}{d_0}. \tag{1}$$

Then, the *true* stress, σ_T, and the *true strain*, ε_T, were computed in terms of the current cross-sectional area, A, and the current marker distance, d, respectively:

$$\sigma_{\mathrm{T}} = \frac{F}{A}, \qquad \varepsilon_{\mathrm{T}} = \int_{d_0}^{d} \frac{\delta d}{d} = \ln \frac{d}{d_0}. \tag{2}$$

Assuming material incompressibility, the *true* data can be related to the *engineering* data as follows:

$$\sigma_{\mathrm{T}} = \sigma_{\mathrm{E}} \left(1 + \varepsilon_{\mathrm{E}}\right) \qquad \varepsilon_{\mathrm{T}} = \ln \left(1 + \varepsilon_{\mathrm{E}}\right). \tag{3}$$

By using Eq. (1) and Eq. (3), the *engineering* and *true* stress-strain curves were plotted for each tested specimen, see for example Figure 5(a). Following the suggestion of [45], the true stress-true strain definition was adopted in the present study. From the stress-strain curve it is possible to identify the following ultimate mechanical properties, see Figure 5(b):

- peak strain, ε_{U}, as the maximum strain before specimen rupture;
- peak stress, σ_{U}, as the maximum stress before specimen rupture;

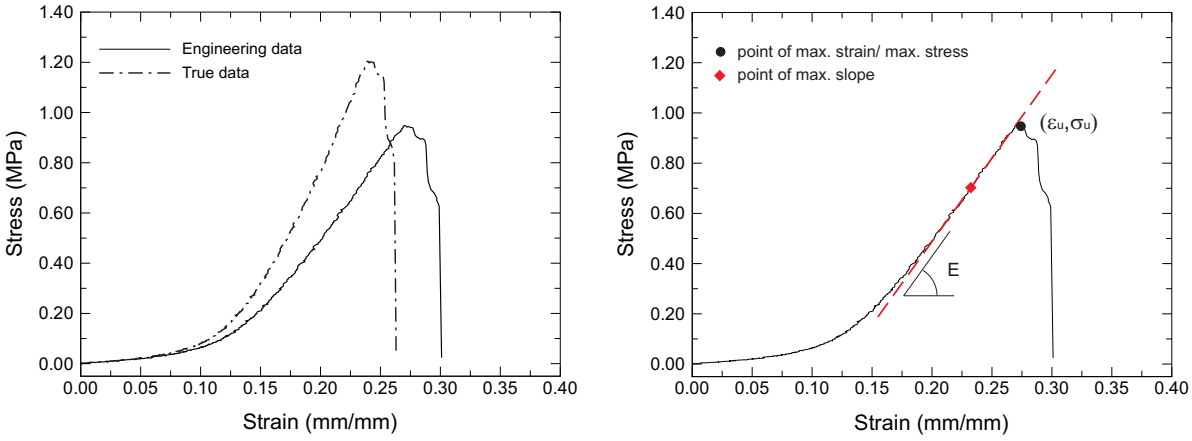

(a) Engineering *vs* true stress-strain curves

(b) Determination of the ultimate mechanical properties

Figure 5: (a) Stress-strain curves computed using both engineering and true stress/strain definitions. (b) Representative stress-strain curve showing the determination of the ultimate mechanical properties (peak strain, peak stress and maximum elastic modulus).

- maximum elastic modulus, $E_{\max}$, as the maximum slope of the stress-strain curve.

Figure 5 highlights that the ultimate mechanical properties are significantly influenced by the different definitions (*engineering* and *true*) of stress and strain. Consequently, it is important to use the same definitions for such quantities to properly compare and interpret the obtained results. A comprehensive discussion on the effect of the different stress/strain definitions is presented in the study of Khanafer *et al.* [45].

2.3.2. Curve fitting and elastic modulus computation

With the aim of computing the elastic modulus as derivative of the stress-strain curve, $\sigma(\varepsilon)$, a simple analytic function can be used. According to [46], curve fittings were obtained by using a polynomial function of the seventh-order:

$$\sigma(\varepsilon) = p_0 + p_1\varepsilon + p_2\varepsilon^2 + p_3\varepsilon^3 + p_4\varepsilon^4 + p_5\varepsilon^5 + p_6\varepsilon^6 + p_7\varepsilon^7, \tag{4}$$

with $p_0, p_1, \ldots, p_7$ stress-like coefficients. For each specimen, the coefficients $p_0, p_1, \ldots, p_7$ were obtained by fitting the polynomial function (4) to each experimental stress-strain curve.

Then, the corresponding analytic function for the elastic modulus, $E(\varepsilon)$, becomes:

$$E(\varepsilon) = \frac{\mathrm{d}\sigma}{\mathrm{d}\varepsilon} = p_1 + 2p_2\varepsilon + 3p_3\varepsilon^2 + 4p_4\varepsilon^3 + 5p_5\varepsilon^4 + 6p_6\varepsilon^5 + 7p_7\varepsilon^6. \tag{5}$$

From the $E(\varepsilon)$ set, the maximum elastic modulus $E_{\max} = \max_{\varepsilon} E(\varepsilon)$ was computed.

2.3.3. Statistical analysis

As previously stated, multiple specimens, circumferentially and longitudinally orientated, were excised from both the anterior and posterior (when possible) samples of each patient. Consequently, multiple values of peak strain, ε_{U}, peak stress, σ_{U}, and maximum elastic modulus, $E_{\max}$ were computed and collected for each patient and combination of region and orientation. Values of the three properties were then averaged to obtain a single representative value for region/orientation of each patient.

The averaged ultimate mechanical properties (ε_{U}, σ_{U} and $E_{\max}$) were subdivided into:

- four groups according to specimen location and orientation, i.e., anterior/circumferential (AC), anterior/longitudinal (AL), posterior/circumferential (PC) and posterior/longitudinal (PL);
- four groups according to patient age (younger, age $\leq$ 52 years and older, age $>$ 52 years)[1] and specimen orientation, i.e., younger/circumferential (YC), younger/longitudinal (YL), older/circumferential (OC) and older/longitudinal (OL).
- four groups according to patient sex and specimen and orientation, i.e., male/circumferential (MC), male/longitudinal (ML), female/circumferential (FC) and female/longitudinal (FL).

Basic statistical analysis (including descriptive, comparative and correlation operations) was performed on the data organized as mentioned above, using the Statistics Toolbox of Matlab R2011. However, before any statistical data elaboration, normal distribution of ε_{U}, σ_{U} and $E_{\max}$ data was verified for each region/orientation group as well as for each age and sex group by using the Kolmogorov-Smirnov test. In the following, descriptive, comparative and correlation statistics is briefly presented.

Descriptive statistics.

For each investigated group, the representative ε_{U}, σ_{U} and $E_{\max}$ of each patient were averaged again. The results are presented as mean ± standard deviation. Since the computation of mean and standard deviation is sensitive to the presence of possible outliers, Grubb's test was used before any averaging with a confidence level of 95%.

Comparative statistics.

A two-sample t-test was used to compare means of two data-sets and then, to determine whether the two

[1] The threshold value of 52 years is the mean between the lower (22 years) and upper (82 years) value of patient age.

means are significantly different. Significance was assumed for a p-value less than 0.05. In particular, the comparisons between two means of a given parameters were performed with respect to:

- the change in orientation for a given region and age/sex group;
- the change in location for a given orientation group;
- the change in age and sex for a given orientation group.

Correlation statistics.

Correlations between two set of data were investigated for each region/orientation and age group to explore whether a relationship between two parameters (chosen between ε_{U}, σ_{U}, E and patient age) takes place or not. In particular, a linear regression analysis was performed to correlate:

- peak stress, σ_{U}, with peak strain, ε_{U}, for a given region/orientation group;
- peak stress, σ_{U}, with elastic modulus, $E_{\max}$, for a given region/orientation group;
- peak stress, σ_{U}, with patient age for a given region/orientation group.

Correlation between two parameters was determined using the Pearson's correlation coefficient (r). Correlations were assumed significant for a p-value less than 0.05. All the obtained results are reported in Section 3.

3. Results

Eighty-six samples of dilated ascending aorta (46 and 39 for the anterior and posterior region, respectively) were obtained from 46 patients (62 ± 14 years; male/female ratio 34/12) who underwent surgical repair. From the 86 samples, 403 specimens were excised for tensile testing. Such aortic specimens were categorized into groups according to region (anterior and posterior) and orientation (circumferential and longitudinal). In particular, 272 specimens for the anterior zone (146 circumferentially-oriented and 126 longitudinally-oriented) and 131 specimens for the posterior zone (74 circumferentially-oriented and 57 longitudinally-oriented) were obtained.

About 39% of the total number of tested specimens (n = 160) was excluded from post-processing because of slippage at the grips, rupture outside the markers and/or low quality of the stress-strain curve. The remaining 61% (n = 247) was considered successful for data and statistical analysis. As previously stated, the multiple value of ε_{U}, σ_{U}, and $E_{\max}$ were properly averaged to have a single representative value for each

region/orientation combination of each patient, obtaining 122 sets of data from 247 initially available.

The averaged mechanical properties (representative of each patient) were collected and summarized in Table 1 for the four region/orientation groups. Figure 6 shows the averaged true stress-true strain curves (representative of each patient) for the four possible combinations of region/orientation. As expected, such sets of curves evidence a nonlinear and anisotropic behavior of the aortic tissue, with large deformation before specimen rupture.

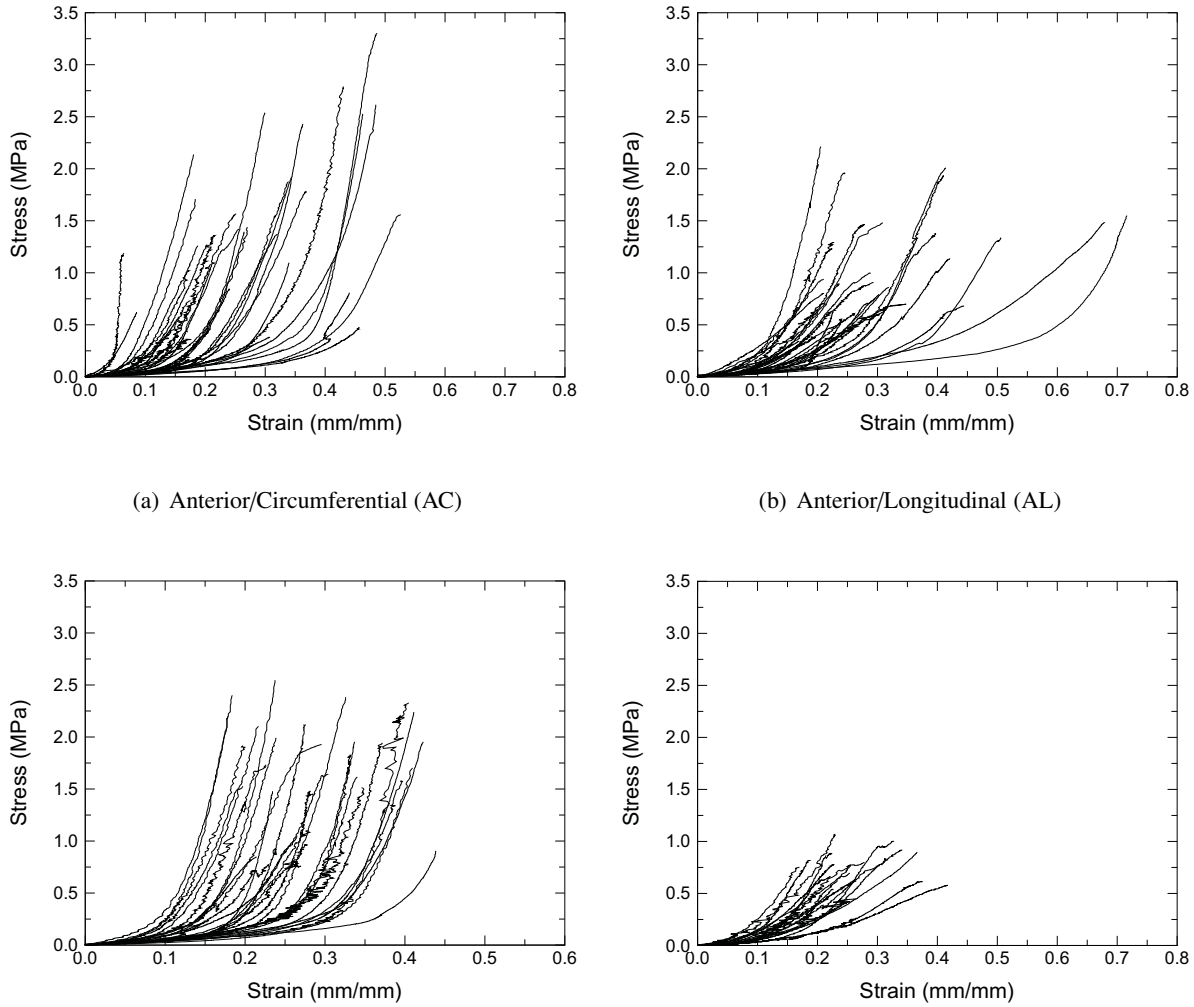

(a) Anterior/Circumferential (AC)

(b) Anterior/Longitudinal (AL)

(c) Posterior/Circumferential (PC)

(d) Posterior/Longitudinal (PL)

Figure 6: True stress-true strain curves of all patients for each region/orientation group: (a) anterior/circumferential (AC), (b) anterior/longitudinal (AL), (c) posterior/circumferential (PC), (d) posterior/longitudinal (PL).

Table 1: Ultimate mechanical properties, ε_U (mm/mm),σ_U (MPa) and E_{max} (MPa), for each patient and region/orientation groups

			AC			AL			PC			PL		
Patient	Gender	Age	ε_U	σ_U	E_{max}	ε_U	σ_U	E_{max}	ε_U	σ_U	E_{max}	ε_U	σ_U	E_{max}
P02	M	76	0.307	0.38	3.10	0.294	0.64	5.60	-	-	-	-	-	-
P03	M	59	0.457	0.48	5.39	0.716	1.55	18.53	-	-	-	-	-	-
P04	M	79	0.392	1.96	29.21	0.226	0.64	13.60	-	-	-	-	-	-
P05	M	52	0.475	3.38	30.42	0.506	1.34	10.16	-	-	-	-	-	-
P06	F	52	0.476	1.78	35.28	0.414	2.01	16.58	0.454	1.91	23.85	-	-	-
P07	M	55	0.441	0.81	15.07	0.444	0.68	4.82	0.439	0.90	16.65	-	-	-
P08	F	81	0.080	0.70	11.82	0.169	0.34	3.67	0.234	1.48	45.03	-	-	-
P10	F	76	0.244	1.20	11.71	0.237	0.90	8.37	-	-	-	-	-	-
P11	F	83	0.156	0.58	8.96	0.210	0.80	5.45	0.185	0.61	9.92	-	-	-
P12	M	23	0.601	2.18	26.74	0.679	1.39	6.79	-	-	-	-	-	-
P13	M	64	-	-	-	-	-	-	0.289	2.18	26.39	0.249	0.57	3.30
P14	M	75	-	-	-	-	-	-	0.380	1.98	35.27	0.254	0.70	4.01
P15	F	46	0.413	1.42	18.35	-	-	-	0.423	1.95	24.54	-	-	-
P16	F	68	0.338	2.01	19.68	0.264	0.48	4.79	0.387	2.81	27.95	-	-	-
P17	M	25	0.484	2.90	(69.15)	-	-	-	-	-	-	-	-	-
P18	M	36	0.396	3.00	46.32	0.424	1.44	12.26	0.495	3.50	60.26	-	-	-
P19	M	49	0.290	1.48	15.27	0.412	1.37	11.57	-	-	-	-	-	-
P20	M	69	0.172	1.98	27.22	0.218	0.72	7.86	0.284	3.74	54.09	0.255	0.76	7.66
P21	M	56	0.339	1.88	16.71	-	-	-	0.296	1.93	17.50	-	-	-
P22	M	52	-	-	-	-	-	-	0.225	1.95	30.66	-	-	-
P24	F	61	0.365	1.45	13.68	0.315	0.63	4.38	0.346	2.03	51.53	0.381	0.45	4.26
P26	F	56	0.336	1.63	23.81	0.228	1.19	12.11	0.277	1.82	36.33	0.296	0.98	8.41
P27	F	64	0.208	0.46	7.61	0.182	0.38	8.35	0.250	0.80	7.62	0.278	0.80	6.08
P28	M	69	0.230	1.49	15.64	0.268	0.57	5.65	0.187	2.47	39.24	0.230	1.07	11.46
P30	M	62	0.171	1.02	18.22	0.247	0.55	3.46	0.315	2.16	26.65	-	-	-
P31	M	67	0.273	1.43	23.16	0.277	0.59	5.78	0.250	1.03	11.39	0.238	0.60	8.88
P32	M	41	0.361	1.80	34.34	0.352	0.97	11.35	0.383	1.67	29.15	0.213	0.97	11.68
P33	M	65	0.271	1.44	18.39	0.309	1.48	11.44	0.278	1.10	12.18	-	-	-
P34	M	76	0.231	0.91	10.57	0.178	0.36	2.59	0.226	1.70	18.24	-	-	-
P35	M	72	0.200	1.20	15.00	0.234	0.69	5.62	0.358	2.13	39.53	0.208	0.37	3.53
P36	M	78	0.185	1.72	19.83	0.195	0.88	9.62	0.243	2.39	35.95	0.170	0.75	8.86
P37	F	73	0.167	0.36	4.50	0.229	0.40	7.08	0.230	0.78	9.55	0.226	0.78	7.38
P38	M	67	0.207	1.25	13.18	0.181	0.37	4.84	0.304	1.64	18.83	0.239	0.64	5.96
P39	M	71	0.239	1.08	16.34	0.359	0.85	4.21	0.295	1.98	31.97	0.366	0.90	5.45
P40	M	69	0.175	0.73	12.24	0.248	1.80	17.80	0.331	1.83	37.98	0.265	0.64	4.27
P41	M	60	-	-	-	0.205	2.21	(29.56)	-	-	-	-	-	-
P42	M	77	0.227	1.34	22.68	0.258	1.07	12.70	0.284	1.44	43.65	0.311	0.83	6.11
P43	M	70	0.202	1.60	19.60	0.340	0.78	4.34	-	-	-	-	-	-
P44	F	74	0.237	1.30	15.11	0.207	0.70	5.98	0.226	1.73	21.07	0.172	0.71	6.76
P45	M	75	0.239	1.20	14.96	-	-	-	0.275	2.12	38.02	0.341	0.92	4.58
P46	M	63	0.268	1.83	20.14	0.222	1.26	11.11	0.405	2.33	49.99	0.387	0.61	3.23

- : no data and/or unsuccessful test; outlier specified in brackets; standard deviation not specified.

Table 2: Influence of region/orientation on peak strain, peak stress and maximum elastic modulus (mean ± standard deviation).

	Anterior		Posterior	
	Circumferential	Longitudinal	Circumferential	Longitudinal
Peak strain (mm/mm)	0.293± 0.117	0.289± 0.110	0.301± 0.090	0.267± 0.065
Peak stress (MPa)	1.44± 0.70	0.94± 0.49	1.85± 0.70	0.74± 0.18
Elastic modulus (MPa)	18.34± 9.00	8.44± 4.23	30.03± 13.85	6.41± 2.58

3.1. Influence of region/orientation on the averaged ultimate mechanical properties

The obtained averaged data ($n = 122$) were subdivided in the following groups: anterior/circumferential, AC, ($n = 37$), anterior/longitudinal, AL, ($n = 34$), posterior/circumferential, PC, ($n = 32$) and posterior/longitudinal, PL, ($n = 19$). The results are presented as mean ± standard deviation and are summarized in Table 2. Bar diagrams of the ultimate mechanical properties (ε_U, σ_U and E_{max}) are shown in Figure 7, as a function of region and orientation.

For the anterior zone, the mean peak strain, ε_U, was 0.293 ± 0.117 in the circumferential direction and 0.289 ± 0.110 in the longitudinal one; while, for the posterior zone, the mean ε_U was 0.301 ± 0.090 and 0.267 ± 0.065, respectively, see Table 2 and Figure 7(a). No significant difference in the mean ε_U was found between the two groups ($p > 0.05$).

For the anterior zone, the mean peak stress, σ_U, was 1.44 ± 0.70 in the circumferential direction and 0.94 ± 0.49 MPa in the longitudinal one; while, for the posterior zone, the (mean) σ_U was 1.85 ± 0.70 and 0.74 ± 0.18 MPa, respectively, see Table 2 and Figure 7(b). The circumferential mean σ_U was significantly higher than the longitudinal one in both anterior ($p = 9.58e-04$) and posterior ($p = 1.76e-08$) region. A significant difference in the mean σ_U was found between anterior and posterior region only for the circumferential direction ($p = 0.018$), with posterior mean σ_U higher than the anterior one. No significant difference was found between anterior and posterior zones for the longitudinal orientation ($p = 0.091$).

For the anterior zone, the mean elastic modulus, E_{max}, was 18.34 ± 9.0 in the circumferential direction and 8.44 ± 4.23 MPa in the longitudinal one; while, for the posterior zone, the mean E_{max} was 30.03 ± 13.85 and 6.41 ± 2.58 MPa, respectively, see Table 2 and Figure 7(c): The circumferential stiffness E_{max} was

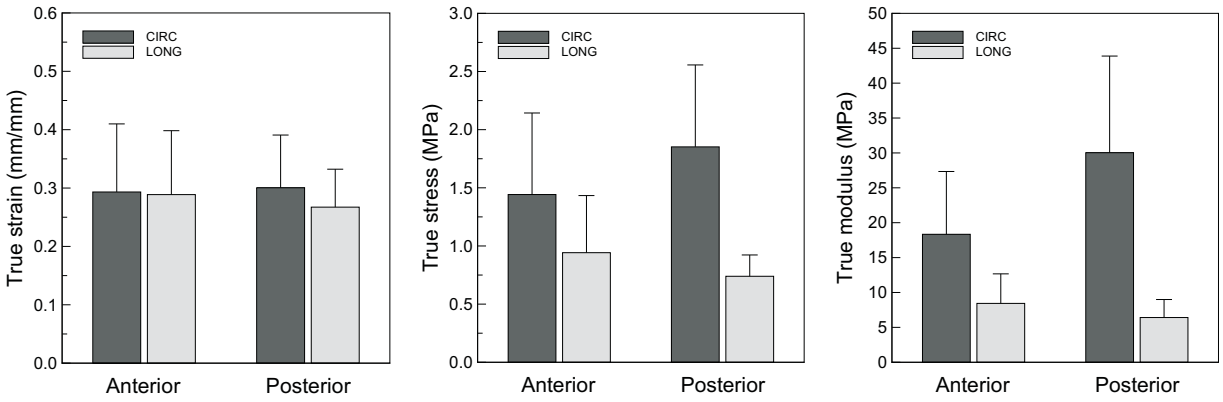

(a) Peak strain (b) Peak stress (c) Max. elastic modulus

Figure 7: Bar diagrams of (a) peak strain, (b) peak stress and (c) maximum elastic modulus as function of region/orientation.

significantly higher than the longitudinal one in both anterior ($p = 1.62e-05$) and posterior ($p = 3.04e-04$) region. A significant difference in the mean $E_{\max}$ was found between anterior and posterior region only for the circumferential direction ($p = 0.009$), with the posterior measured value higher than the anterior one. No significant difference was found between anterior and posterior zones for the longitudinal orientation($p = 0.056$).

3.2. Influence of age/orientation on the average ultimate mechanical properties

The obtained averaged data ($n = 122$) were subdivided in the following groups: young/circumferential, YC, ($n = 13$), young/longitudinal, YL, ($n = 56$), old/circumferential, OC, ($n = 7$) and old/longitudinal, OL, ($n = 46$). The results are presented as mean ± standard deviation and are summarized in Table 3. Bar diagrams of the ultimate mechanical properties (ε_U, σ_U and $E_{\max}$) are shown in Figure 8, as a function of age and orientation.

For the young-aged group, the mean peak strain, ε_U, was 0.421 ± 0.096 in the circumferential direction and 0.429 ± 0.142 in the longitudinal one; while, for the old-aged group, the (mean) ε_U was 0.268 ± 0.084 and 0.258 ± 0.063, respectively, see Table 3 and Figure 8(a). No significant difference in the ultimate strain value was found between the two groups ($p > 0.05$).

For the young-aged group, the mean peak stress, σ_U, was 2.23 ± 0.10 in the circumferential direction and 1.25 ± 0.14 in the longitudinal one; while, for the old-aged group, the mean σ_U was 1.45 ± 0.59 and

Table 3: Influence of age/orientation on peak strain, peak stress and maximum elastic modulus (mean ± standard deviation).

	Young		Old	
	Circumferential	Longitudinal	Circumferential	Longitudinal
Peak strain (mm/mm)	0.421± 0.096	0.429± 0.142	0.268± 0.084	0.258± 0.063
Peak stress (MPa)	2.23± 0.10	1.25± 0.14	1.45± 0.59	0.76± 0.31
Elastic modulus (MPa)	34.18± 15.72	11.48± 2.90	22.11± 12.55	7.11± 3.63

0.76 ± 0.31, respectively, see Table 3 and Figure 8(b). The circumferential mean σ_U was significantly higher than the longitudinal one for both young-aged ($p = 0.008$) and old-aged ($p = 6.38e-09$) group. The mean σ_U was significantly higher in the young-aged group than the old-aged group for both circumferential ($p = 7.63e-04$) and longitudinal ($p = 5.64e-04$) direction.

For the young-aged group, the (mean) elastic modulus, E_{max}, was 34.18 ± 15.72 in the circumferential direction and 11.48 ± 2.90 in the longitudinal one; while, for the old-aged group, the (mean) E_{max} was 22.11 ± 12.55 and 7.11 ± 3.63, respectively, see Table 3 and Figure 8(c). The circumferential (mean) E_{max} was significantly higher than the longitudinal one for both the young-aged ($p = 0.0015$) and old-aged ($p = 1.852e-05$) groups. Both circumferential and longitudinal (mean) E_{max} were higher in the young-aged than in the old-aged group, respectively, but such a difference was weakly significant in the longitudinal direction ($p = 0.048$) and no significant in the circumferential direction.

3.3. Influence of sex/orientation on the average ultimate mechanical properties

The obtained averaged data ($n = 122$) were subdivided in the following groups: male/circumferential, MC, ($n = 47$), male/longitudinal, ML, ($n = 38$), female/circumferential, FC, ($n = 22$) and female/longitudinal, OL, ($n = 15$). The results are presented as mean ± standard deviation and are summarized in Table 4. Bar diagrams of the ultimate mechanical properties (ε_U, σ_U and E_{max}) are shown in Figure 9, as a function of sex and orientation.

For males, the mean peak strain, ε_U, was 0.299 ± 0.089 in the circumferential direction and 0.292 ± 0.102 in the longitudinal one; while, for females, it measured 0.277 ± 0.115 and 0.254 ± 0.073, respectively, see Table 4 and Figure 9(a): No significant difference in the mean ε_U was found between the two groups.

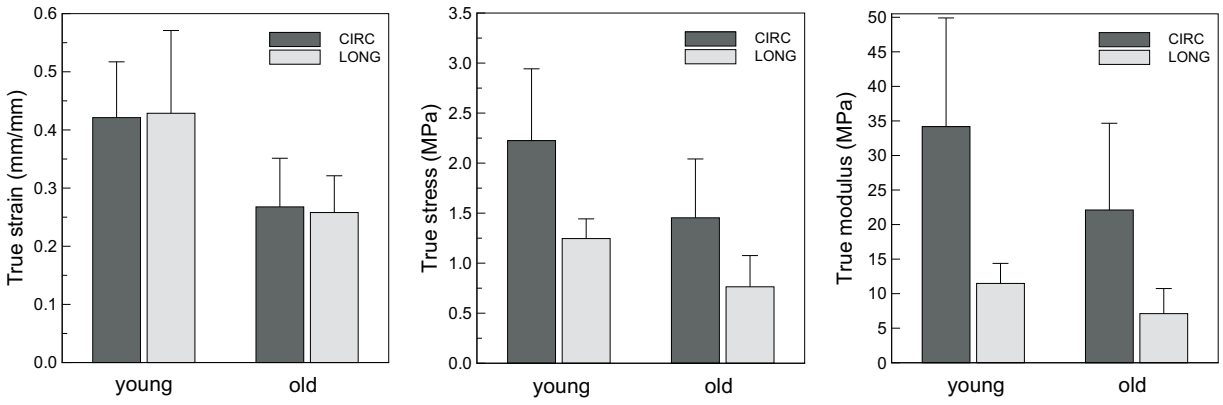

(a) Peak strain (b) Peak stress (c) Max. elastic modulus

Figure 8: Bar diagrams of (a) peak strain, (b) peak stress and (c) maximum elastic modulus as function of age/orientation.

Table 4: Influence of sex/orientation on peak strain, peak stress and maximum elastic modulus (mean ± standard deviation).

	Male		Female	
	Circumferential	Longitudinal	Circumferential	Longitudinal
Peak strain (mm/mm)	0.299± 0.089	0.292± 0.102	0.277± 0.115	0.254± 0.073
Peak stress (MPa)	1.76± 0.09	0.87± 0.10	1.36± 0.63	0.68± 0.24
Elastic modulus (MPa)	25.29± 12.74	7.86± 4.02	20.38± 12.56	6.65± 2.15

For males, the mean peak stress, σ_{U}, was 1.76 ± 0.09 in the circumferential direction and 0.87 ± 0.10 in the longitudinal one; while, for females, the mean σ_{U} was 1.36 ± 0.63 and 0.68 ± 0.24, respectively, see Table 4 and Figure 9(b). The circumferential mean σ_{U} was significantly higher than the longitudinal one for both the male ($p = 1.31e - 08$) and female ($p = 0.0031$) groups. Both circumferential and longitudinal mean $E_{\max}$ was higher for males than females, respectively, but such a difference was significant only for the circumferential direction ($p = 0.034$).

For males, the mean peak stress, $E_{\max}$, was 25.29 ± 12.74 in the circumferential direction and 7.86 ± 4.02 in the longitudinal one; while, for females, the measured value $E_{\max}$ was 20.38 ± 12.56 and 6.65 ± 2.15, respectively (see Table 4 and Figure 9(c)). The circumferential (mean) $E_{\max}$ was higher than the longitudinal

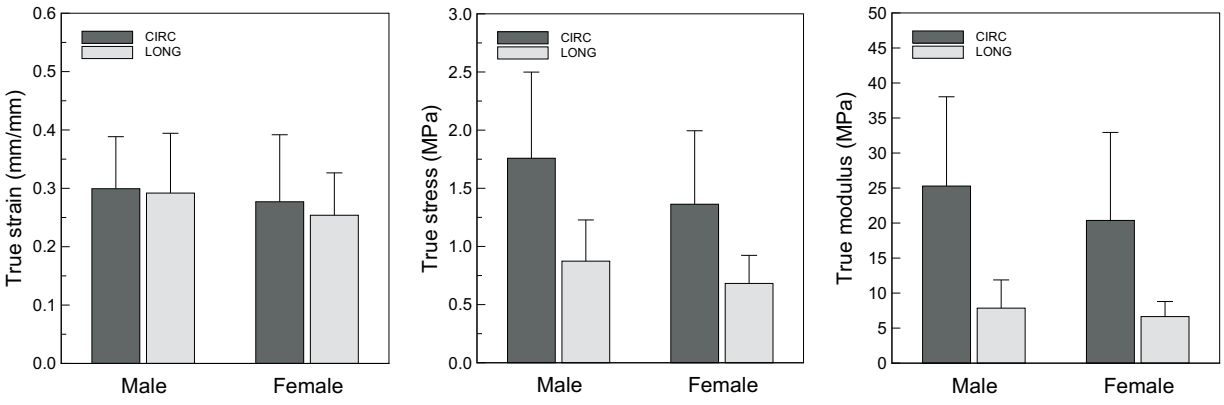

(a) Peak strain (b) Peak stress (c) Max elastic modulus

Figure 9: Bar diagrams of (a) peak strain, (b) peak stress and (c) maximum elastic modulus as function of sex/orientation.

one, with an high significant difference for males ($p = 1.71e-10$) and a weak significant difference for female patients ($p = 0.046$). No significant difference in the tissue stiffness was found between male and female groups in both the circumferential and longitudinal directions.

3.4. Ultimate mechanical properties and age correlations

Figures 10-12 show, for each region and orientation group, linear regression plots between peak stress *vs* peak strain, maximum elastic modulus and patient age, respectively.

For the anterior/circumferential group, peak stress was weakly (significantly) correlated with peak strain, $\sigma_U = 3.2\varepsilon_U + 0.49$ ($r = 0.537, p = 0.001$); strongly (significantly) correlated with maximum elastic modulus, $\sigma_U = 0.047E_{max} + 0.52$ ($r = 0.820$, $p = 5.39 - e10$), and weakly (significantly) with patient age $\sigma_U = -0.028\text{age} + 3.2$ ($r = -0.586$, $p = 1.37 - e04$), see Figure 10.

For the anterior/longitudinal group, peak stress was weakly (significantly) correlated with peak strain, $\sigma_U = 1.7\varepsilon_U + 0.44$ ($r = 0.448$, $p = 0.008$); strongly (significantly) correlated with maximum elastic modulus, $\sigma_U = 0.074E_{max} + 0.27$ ($r = 0.841$, $p = 4.58e - 10$), and weakly (significantly) with patient age, $\sigma_U = -0.018\text{age} + 2.1$ ($r = -0.487$, $p = 0.003$), see Figure 11.

For the anterior/circumferential group, peak stress was weakly (significantly) correlated with peak strain, $\sigma_U = 3.0\varepsilon_U + 0.95$, ($r = 0.383, p = 0.030$), see Figure 12. No correlation was found between peak stress and maximum elastic modulus ($r = 0.164$, $p = 0.370$) as well as between peak stress and patient age

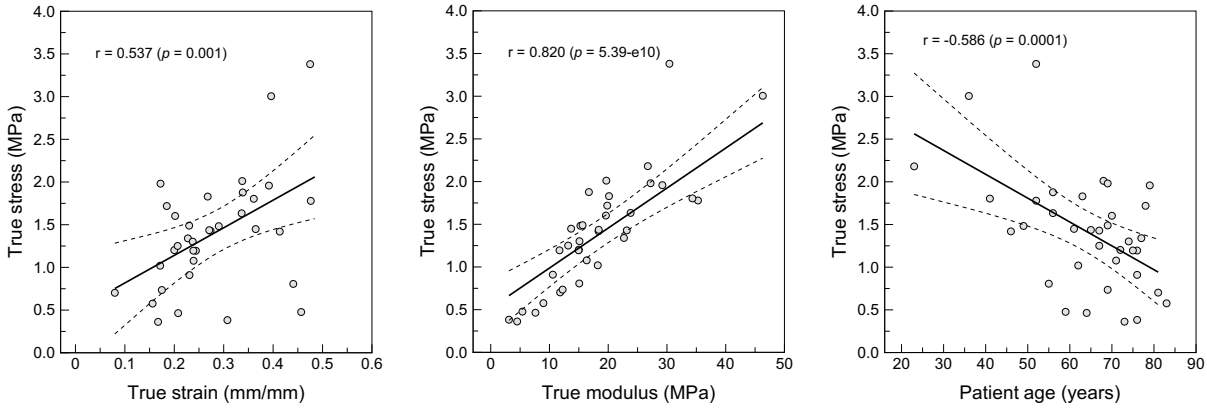

(a) (b) (c)

Figure 10: Anterior/circumferential group: correlations between (a) peak stress and peak strain ($r = 0.537$, $p = 0.001$), (b) peak stress and maximum elastic modulus ($r = 0.820$, $p = 5.39 - e10$),and (c) peak stress and patient age ($r = -0.586$, $p = 0.0001$). Continuous lines show linear fits to data sets and dashed lines the confidence intervals (95%) of the regression lines.

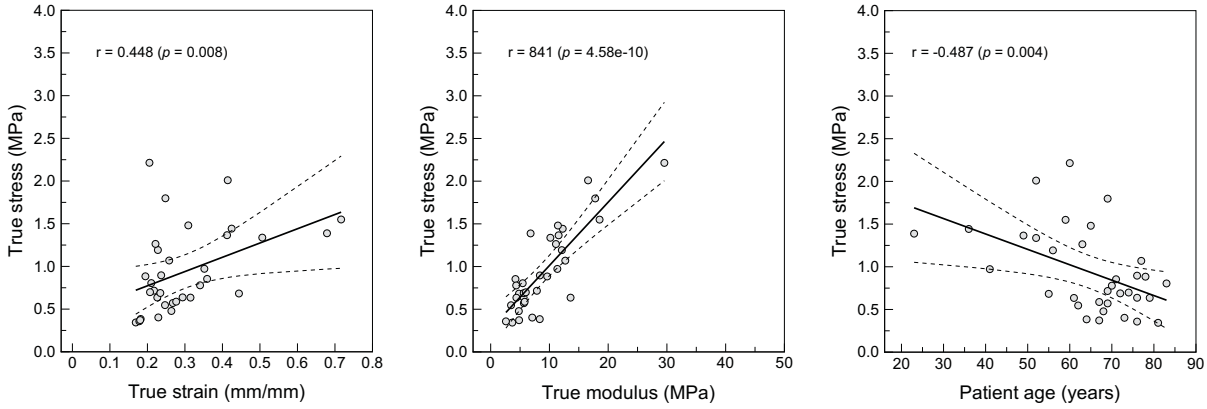

(a) (b) (c)

Figure 11: Anterior/longitudinal group: correlations between (a) peak stress and peak strain ($r = 0.448$, $p = 0.008$), (b) peak stress and maximum elastic modulus ($r = 0.841$, $p = 4.58e - 10$),and (c) peak stress and patient age ($r = -0.487$, $p = 0.003$). Continuous lines show linear fits to data sets and dashed lines the confidence intervals (95%) of the regression lines.

($r = -0.260$, $p = 0.149$).

For the anterior/circumferential group, peak stress, σ_U, was (significantly) correlated with maximum elastic

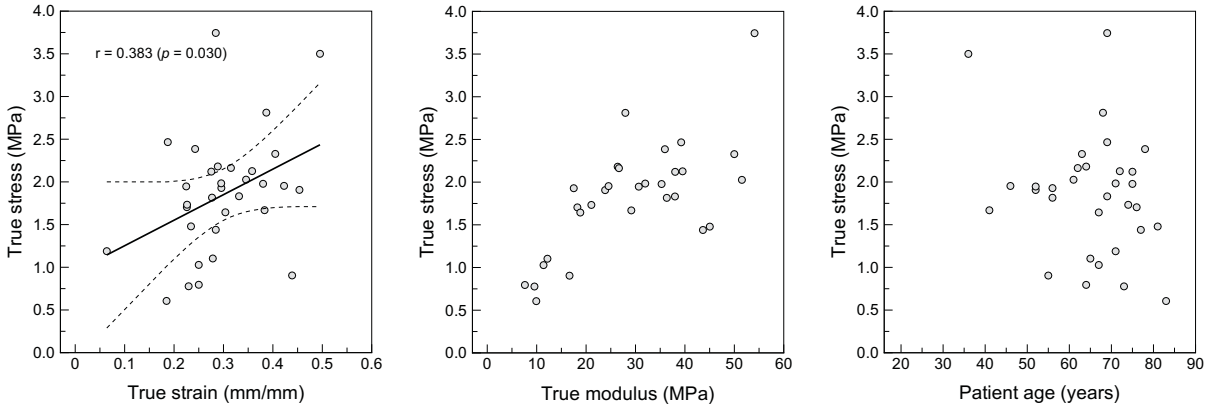

(a) (b) (c)

Figure 12: Posterior/circumferential group: correlations between (a) peak stress and peak strain ($r = 0.383$, $p = 0.030$), (b) peak stress and maximum elastic modulus ($r = 0.164$, $p = 0.370$),and (c) peak stress and patient age ($r = -0.260$, $p = 0.149$). Continuous lines show linear fits to data sets and dashed lines the confidence intervals (95%) of the regression lines.

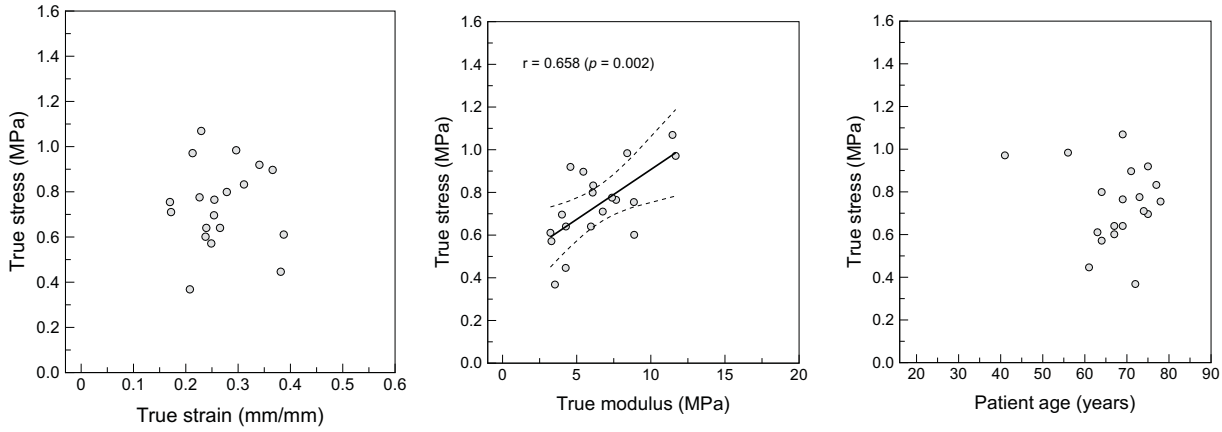

(a) (b) (c)

Figure 13: Posterior/longitudinal group: correlations between (a) peak stress and peak strain ($r = -0.005$, $p = 0.985$), (b) peak stress and maximum elastic modulus ($r = 0.658$, $p = 0.002$),and (c) peak stress and patient age ($r = -0.162$, $p = 0.507$). Continuous lines show linear fits to data sets and dashed lines the confidence intervals (95%) of the regression lines.

modulus, $E_{\max}$, $\sigma_{\mathrm{U}} = 0.05E_{\max} + 0.44$ ($r = 0.658$, $p = 0.002$), see Figure 13. No correlation was found between peak stress and both peak strain ($r = -0.005$, $p = 0.985$) and patient age ($r = -0.162$, $p = 0.507$).

4. Discussion

The present work deals with the study of dilated ascending aorta with the aim of evaluating the ultimate mechanical properties of asAA tissues. In particular, uniaxial tests were performed on specimens excised from patients who underwent open-heart elective AsAA surgery. The specimens, circumferentially and longitudinally oriented, were cut from the anterior and posterior region (when possible) of the excised aortic portion. The peak strain, peak stress and maximum elastic modulus were detected from true stress-true strain curves and, then, collected and statistically analyzed to highlight the effect of specimen location and orientation as well as patient age and sex on the measured mechanical properties.

To the authors' knowledge, the mechanical properties of the ascending aorta have been studied by different researchers using both uniaxial [28, 31, 35–37, 39] and biaxial tensile tests [29, 30, 32, 34, 42]. In the following, a discussion of our results in terms of true-strain and true-stress is presented, and integrated by a comparison with the most significant results available in the literature.

Influence of region and orientation

Our results confirm the anisotropy of the dilated aortic tissue, with values of strength (i.e., peak stress) and stiffness (i.e., maximum elastic modulus) significantly higher in the circumferential than in the longitudinal direction. Such differences were not observed for the peak strain. Our results are consistent with many of the previous studies available in the literature, as the recent works of Duprey *et al.* [36], Khanafer *et al.* [37], Pham *et al.* [42] and Pichamuthu *et al.* [43], whereas disagree with the results of Vorp *et al.* [31], which found non-significant difference between the two orientations.

According to our results, significant difference was also observed in the ultimate mechanical properties between the two region groups (anteriori vs posterior). In particular, higher values of strength and stiffness were found in the posterior zone than in anterior one for the circumferential direction. On the contrary, lower values of strength and stiffness were found in the posterior than in the anterior region for the longitudinal direction, but such differences were not significant. For the sake of comparison, in the literature, Duprey *et al.* [36] and Khanafer *et al.* [37] found that the posterior region was significantly stiffer than the anterior one only in the longitudinal direction, whereas Choudhury *et al.* [34] found that the posterior zone was stiffer than the anterior one for both orientations, but without statistic significance. Iliopoulos *et al.* [35] besides the anterior and posterior region considered also the two lateral parts. Their results indicated regional variation in strength and stiffness with the lowest value in the anterior region. Finally, no significant difference in

tissue stiffness was found by Azadani *et al.* [47] between anterior and posterior regions of the ascending aorta.

Influence of patient age

Our results evidenced that peak strain, peak stress and maximum elastic modulus of AsAA tissues significantly decrease with patient age for both circumferential and longitudinal orientation. A negative correlation of peak stress with age was found to be significant in all anterior groups, whereas no correlation was found in the posterior ones (with the only exception for the stress-strain correlation in the PC group).

The influence of aging on the mechanical properties of the aortic tissue has been studied in few works available in the literature [25, 38, 39]. In agreement with our results, a negative correlation of peak stress with aging was also found by Okamoto *et al.* [25] for dilated ascending aorta, as well as by Groenink *et al.* [38] and Guinea *et al.* [39] for healthy descending thoracic aorta. On the contrary, Khanafer *et al.* [37] did not found any correlation between peak stress and age for dilated ascending aorta.

It is worth noting that Guinea and co-workers also observed that peak stress and peak strain fell drastically beyond the age of 30 years, and that aortic tissue became more isotropic with aging. Such finding are not in agreement with our results, for which the anisotropic behavior was observed in both the younger and older patients.

Influence of patient sex

To the authors' knowledge, few works aiming to study the dependency of mechanical properties of AsAA on sex are available in the literature. Our results evidenced significant differences in the peak stress between males and females only in the circumferential direction. Similar findings were also observed by Sokolis and Iliopoulos [40] for dilated ascending aorta as well as by Guinea *et al.* [39] for healthy descending aorta.

Limitation and future developments

The main goal of the present study was to improve the knowledge on AsAA tissue from the mechanical point of view, presenting results of uniaxial tests performed on a considerable number of human specimens. However, patient-specific data on concomitant pathologies which could contribute to the dilation of the aortic wall were not included in our study and correlated with our experimental findings.

In particular, no information were provided about the possible concomitant presence of bicuspid aortic valve (BAV), which is thought to be correlated with an increasing wall stiffness [36, 41–44], and/or other co-morbidities in AsAA patients. No comparison between normotensive and hypertensive AsAA patients were performed. A relationship between increased aortic stiffness and blood pressure is suggested in the literature [34, 37, 42], where increased systolic pressure may be an initial cause of tissue stiffening.

As previously stated, our study focused on the mechanical characterization of the AsAA tissue. A comparison between histological and bio-mechanical properties of pathological and healthy aortic tissues should be also examined to understand possible alterations in the micro-structure and then in the modification of bio-mechanical behavior of aortic tissues [31, 41, 48].

Moving from such considerations, with the aim of improving the knowledge of AsAA, future developments of the present work should integrate the obtained mechanical data with clinical, histological and genetic data of the investigated AsAA patients, as well as with information extracted from medical images such as, for example, aortic compliance.

5. Conclusions

Forty-six patients with dilated ascending aorta who underwent elective AsAA surgical repair were included in the present study. Specimens, circumferentially and longitudinally oriented, were obtained from the anterior and posterior region (when possible) of tubular-shaped portions of dilated aorta excised through open-heart surgery. Uniaxial tensile tests were performed with the aim of evaluating the ultimate mechanical properties of AsAA tissues: The peak strain, peak stress and maximum elastic modulus were detected from true stress- true strain curves and, then, collected and statistically analyzed to highlight the effect of specimen location and orientation as well as patient age and sex.

To know when complications (dissection/rupture) of thoracic aortic aneurysm occur would permit rational decision-making process, regarding elective, preemptive surgical intervention. The present work aimed at representing a contribution to the study of aneurysm evolution till rupture through the analysis of measured mechanical properties of the pathologic tissue excised from a considerable number of patients.

Acknowledgments

It is gratefully acknowledged the support of: MIUR organization through the Project no. 2010BFXRHS, and ERC

Starting Grant through the Project ISOBIO: Isogeometric Methods for Biomechanics (No. 259229).

References

[1] A. Evangelista, Aneurysm of the ascending aorta, Heart 96 (2010) 979–985.

[2] D. Lavall, H. J. Schafers, M. Bohm, U. Laufs, Aneurysms of the ascending aorta, Deutsches Arzteblatt International 109 (2012) 227–233.

[3] W. D. Clouse, J. W. J. Hallett, H. V. Schaff, M. M. Gayari, D. M. Ilstrup, L. J. M. 3rd, Improved prognosis of thoracic aortic aneurysms: a population-based study, JAMA 280 (1998) 1926–1929.

[4] J. M. Ruddy, J. A. Jones, F. G. Spinale, J. S. Ikonomidis, Regional heterogeneity within the aorta: relevance to aneurysm disease, The Journal of Thoracic and Cardiovascular Surgery 136 (2008) 1123–1130.

[5] A. M. Booher, K. A. Eagle, Diagnosis and management issues in thoracic aortic aneurysm, American Heart Journal 162 (2011) 38–46.

[6] V. L. Gott, P. S. Greene, D. E. Alejo, D. E. Cameron, D. C. Naftel, D. C. Miller, A. M. Gillinov, J. C. Laschinger, R. E. Pyeritz, Replacement of the aortic root in patients with marfans syndrome, The New England Journal of Medicine 340 (1999) 1307–1313.

[7] B. S. Brooke, J. P. Habashi, D. P. Judge, N. Patel, B. Loeys, H. C. D. 3rd, Angiotensin ii blockade and aortic-root dilation in marfans syndrome, The New England Journal of Medicine 358 (2010) 2787–2795.

[8] J. H. Lindeman, B. A. Ashcroft, J. W. Beenakker, M. van Es, N. B. Koekkoek, F. A. P. J. F. Tielemans, H. Abdul-Hussien, R. A. Bank, T. H. Oosterkamp, Distinct defects in collagen microarchitecture underlie vessel-wall failure in advanced abdominal aneurysms and aneurysms in marfan syndrome, Proceedings of the National Academy of Sciences of the United States of America 107 (2010) 862–865.

[9] L. C. Chu, P. T. Johnson, H. C. Dietz, B. S. Brooke, G. J. Arnaoutakis, J. H. B. III, E. K. Fishman, Vascular complications of ehlersdanlos syndrome: Ct findings, American Journal of Roentgenology 198 (2012) 482–487.

[10] K. Hamaoui, A. Riaz, A. Hay, A. Botha, Massive spontaneous diaphragmatic rupture in ehlersdanlos syndrome, Annals of The Royal College of Surgeons of England 94 (2012) e5–e7.

[11] T. Tadros, M. Klein, O. M. Shapira, Ascending aortic dilatation associated with bicuspid aortic valve. pathophysiology, molecular biology, and clinical implications, Circulation 119 (2009) 880–890.

[12] E. Bilen, M. Akcay, N. A. Bayram, U. Kocak, M. Kurt, I. H. Tanboga, E. Bozkurt., Aortic elastic properties and left ventricular diastolic function in patients with isolated bicuspid aortic valve, The Journal of Heart Valve Disease 21 (2012) 189–194.

[13] B. R. Plaisance, M. A. Winkler, A. K. Attili, V. L. Sorrell, Congenital bicuspid aortic valve first presenting as an aortic aneurysm, Am. J. Med. 125 (2012) e5–e7.

[14] S. Verma, S. Siu, Aortic dilatation in patients with bicuspid aortic valve, The New England Journal of Medicine 370 (2014) 1920–1929.

[15] O. E. Dapunt, J. D. Galla, A. M. Sadeghi, S. L. Lansman, C. K. Mezrow, R. A. de Asla, C. Quintana, S. Wallenstein, A. M. Ergin, R. B.Griepp, The natural history of thoracic aortic aneurysms, The Journal of Thoracic and Cardiovascular Surgery 107 (1994) 1323–1332.

[16] N. T. Kouchoukos, D. Dougenis, Surgery of the thoracic aorta, The New England Journal of Medicine 336 (1997) 1876–1888.

[17] J. A. Elefteriades, Natural history of thoracic aortic aneurysms: indications for surgery, and surgical versus nonsurgical risks, The Annals of Thoracic Surgery 74 (2002) S1877–S1880.

[18] J. A. Elefteriades, E. A. Farkas, Thoracic aortic aneurysm clinically pertinent controversies and uncertainties, Journal of the American College of Cardiology 55 (2010) 841–857.

[19] R. R. Davies, L. J. Goldstein, M. A. Coady, S. L. Tittle, J. A. Rizzo, G. S. Kopf, J. A. Elefteriades, Yearly rupture or dissection rates for thoracic aorticaneurysms: simple prediction based on size, The Annals of Thoracic Surgery 73 (2002) 17–28.

[20] L. A. Pape, T. T. Tsai, et al., International registry of acute aortic dissection (irad) aortic diameter 5.5 cm is not a good predictor of type a aortic dissection: observations from the international registry of acute aortic dissection (irad), Circulation 116 (2007) 1120–1127.

[21] C. M. He, M. R. Roach, The composition and mechanical properties of abdominal aortic aneurysms, Journal of Vascular Surgery 20 (1994) 6–13.

[22] P. C. Tang, M. A. Coady, C. Lovoulos, A. Dardik, M. Aslan, J. A. Elefteriades, et al., Hyperplastic cellular remodeling of the media in ascending thoracic aortic aneurysms, Circulation 112 (2005) 1098–1105.

[23] D. C. Iliopoulos, E. P. Kritharis, A. T. Giagini, S. A. Papadodima, D. P. Sokolis, Ascending thoracic aortic aneurysms are associated with compositional remodeling and vessel stiffening but not weakening in age-matched subjects, Journal of Thoracic and Cardiovascular Surgery 137 (2009) 101–109.

[24] A. Tsamis, J. T. Krawiec, D. A. Vorp, Elastin and collagen fibre microstructure of the human aorta in ageing and disease: a review, Journal of the Royal Society Interface 10 (2013) 20121004.

[25] R. J. Okamoto, H. Xu, N. T. Kouchoukos, M. R. Moon, T. M. Sundt, The influence of mechanical properties on wall stress and distensibility of the dilated ascending aorta, The Journal of Thoracic and Cardiovascular Surgery 126 (2003) 842–850.

[26] F. Bonnier, S. Rubin, L. Ventéo, C. M. Krishna, M. Pluot, B. Baehrel, M. Manfait, G. D. Sockalingum, In-vitro analysis of normal and aneurismal human ascending aortic tissues using ft-ir microspectroscopy, Biochimica et Biophysica Acta 1758 (2006) 968–973.

[27] S. Rubin, F. Bonnier, C. Sandt, L. Ventéo, M. Pluot, B. Baehrel, M. Manfait, G. D. Sockalingum, Analysis of structural changes in normal and aneurismal human aortic issues using ftir microscopy, Biopolymers 89 (2008) 160–169.

[28] D. Mohan, J. Melvin, Failure properties of passive human aortic tissue. i-uniaxial tension tests, Journal of Biomechanics 15 (1982) 887–902.

[29] D. Mohan, J. Melvin, Failure properties of passive human aortic tissue. ii-biaxial tension tests, Journal of Biomechanics 16 (1983) 31–44.

[30] R. J. Okamoto, J. E. Wagenseil, W. R. DeLong, S. J. Peterson, N. T. Kouchoukos, T. M. Sundt, Mechanical properties of dilated human ascending aorta, Annals of Biomedical Engineering 30 (2002) 624–635.

[31] D. A. Vorp, B. J. Schiro, M. P. Ehrlich, T. S. Juvonen, M. A. Ergin, B. P. Griffith, Effect of aneurysm on the tensile strength and biomechanical behavior of the ascending thoracic aorta, The Annals of Thoracic Surgery 75 (2003) 1210–1214.

[32] T. Matsumoto, T. Fukui, T. Tanaka, N. Ikuta, T. Ohashi, K. Kumagai, H. Akimoto, K. Tabayashi, M. Sato, Biaxial tensile propertiesof thoracic aortic aneurysm tissues, Journal of Biomechanical Science and Engineering 4 (2009) 518–529.

[33] C. M. García-Herrera, J. M. Atienza, F. J. Rojo, E. Claes, G. V. Guinea, D. J. Celentano, C. García-Montero, R. L. Burgos, Mechanical behaviour and rupture of normal and pathological human ascending aortic wall, Medical & Biological Engineering & Computing 50 (2012) 559–566.

[34] N. Choudhury, O. Bouchot, L. Rouleau, et al., Local mechanical and structural properties of healthy and diseased human ascending aorta tissue, Cardiovascular Pathology 18 (2009) 83–91.

[35] D. C. Iliopoulos, R. P. Deveja, E. P. Kritharis, Regional and directional variations in the mechanical properties of ascending thoracic aortic aneurysms, Medical Engineering & Physics 31 (2009) 1–9.

[36] A. Duprey, K. Khanafer, M. Schlicht, S. Avril, D. Williams, R. Berguer, In vitro characterization of physiological and maximum elastic modulus of ascending thoracic aortic aneurysm using uniaxial tensile testing, European Journal of Vascular and Endovascular Surgery 39 (2010) 700–707.

[37] K. Khanafer, A. Duprey, M. Zainal, M. Schlicht, D. Williams, R. Berguer, Determination of the elastic modulus of ascending thoracic aortic aneurysm at different ranges of pressure using uniaxial tensile testing, The Journal of Thoracic and Cardiovascular Surgery 142 (2011) 682–686.

[38] M. Groenink, S. E. Langerak, E. Vanbavel, E. E. van der Wall, B. J. M. Mulder, A. C. van der Wal, et al., The influence of aging and aortic stiffness on permanent dilation and breaking stress of the thoracic descending aorta, Cardiovascular Research 43 (1999) 471–480.

[39] G. V. Guinea, J. Atienza, F.Rojo, C.Herrera, L. Yiqun, E. Claes, J. Goicolea, C. Montero, R. L. Burgos, F. J. Goicolea, M. Elices., Factors inuencing the mechanical behaviour of healthy human descending thoracic aorta, Physiological measurement 31 (2010) 1553–1565.

[40] D. P. Sokolis, D. C. Iliopoulos, Impaired mechanics and matrix metalloproteinases/inhibitors expression in female ascending thoracic aortic aneurysms, Journal of the mechanical behavior of biomedical materials 34 (2014) 154–164.

[41] S. Pasta, J. A. Phillippi, T. G. Gleason, D. A. Vorp, Effect of aneurysm on the mechanical dissection properties of the human ascending thoracic aorta, The Journal of Thoracic and Cardiovascular Surgery 143 (2012) 460–467.

[42] T. Pham, C. Martin, J. Elefteriades, W. Sun, Biomechanical characterization of ascending aortic aneurysm with concomitant bicuspid aortic valve and bovine aortic arch, Acta Biomaterialia 9 (2013) 7927–7936.

[43] J. E. Pichamuthu, J. A. Phillippi, D. Cleary, D. Chew, J. Hempel, D. A. Vorp, T. Gleason, Differential tensile strength and collagen composition in ascending aortic aneurysms by aortic valve phenotype, The Annals of Thoracic Surgery 96 (2013) 2147–2154.

[44] C. Forsell, J. Swedenborg, J. Roy, T. C. Gasser, Biomechanical properties of the thoracic aneurysmal wall: differences between bicuspid aortic valve and tricuspid aortic valve patients, Annals of Biomedical Engineering 98 (2014) 65–71.

[45] K. Khanafer, M. Schlicht, R. Berguer, How should we measure and report elasticity in aortic tissue?, European Society for Vascular Surgery 45 (2013) 332–339.

[46] D. P. Sokolis, H. Boudoulas, P. E. Karayannacos, Journal of biomechanics, Assessment of the aortic stressstrain relation in uniaxial tension 35 (2002) 1213–1223.

[47] A. N. Azadani, S. Chitsaz, P. B. Matthews, N. Jaussaud, J. Leung, T. Tsinman, L. Ge, E. E. Tseng, Comparison of mechanical properties of human ascending aorta and aortic sinuses, The Annals of Thoracic Surgery 93 (2012) 87–94.

[48] A. N. Azadani, S. Chitsaz, A. Mannion, A. Mookhoek, A. Wisneski, J. M. Guccione, M. D. Hope, L. Ge, E. E. Tseng, Biomechanical properties of human ascending thoracic aortic aneurysm, The Annals of Thoracic Surgery 96 (2013) 50–58.